Progress In Electromagnetics Research M, Vol. 11, 111–122, 2010

ELECTROMAGNETIC BAND GAP STRUCTURES INCORPORATE WITH DUAL BAND MICROSTRIP ANTENNA ARRAY

T. Masri, M. K. A. Rahim, O. Ayop, F. Zubir, N. A. Samsuri and H. A. Majid

Faculty of Electrical Engineering
Radio Communication Engineering Department (RaCED)
Universiti Teknologi Malaysia
Skudai, Johor Bahru 81310, Malaysia

Abstract—A Dual band Microstrip Antenna Arrays (DbMSAA) incorporated with Mushroom Electromagnetic band Gap (MEBG) and modified Minkowski Electromagnetic Band Gap structures to further improve its radiation characteristics is reported in this work. The two different types of EBG structures work like a Band Rejecter (BR), separating the branch of feed line feeding two different groups of patch antenna arrays operating at 2.4 GHz and 5.8 GHz, thus making them operate individually at their particular frequencies, simultaneously. Initially, the possibilities of having a uniform and controlled radiation patterns are quite complicated to achieve due to the single port feeding technique used and developments of grating lobes at the higher band frequency, but, through the incorporation of the EBG structures, the problems could be solved immediately. The antenna's performance is improved where the grating lobes at 5.8 GHz are diminished, and the radiation patterns of the dual band antenna at both frequencies become more symmetrical with increased gain.

1. INTRODUCTION

The next generation wireless communication systems' applications, especially the IEEE 802.11n systems, require at least two antennas to transmit and receive signals, simultaneously. These antennas need to be isolated and separated electrically from one another while maintaining their size as small and as compact as possible. When two different types or shapes of radiating elements working at two

---

Corresponding author: M. K. A. Rahim (mkamal@fke.utm.my).

different frequencies of operation are being integrated as one array formation, the possibilities of having a uniform and controlled radiation patterns are quite tricky to achieve. For microstrip patch type of antennas, other than the existence of mutual couplings among these patches and the others acting as parasitic elements when not resonating, one of the contributing factors to this drawback is that the lower band radiating elements sometimes demonstrate higher (harmonics) resonant frequencies, and if it happens to resonate at the intended second band of frequency of operation at a different phase, this will probably degrade the antennas' radiation patterns. This occurs in the DbMSAA designed in this work, and in [1] a novel and innovative technique to solve the intricacy is introduced by

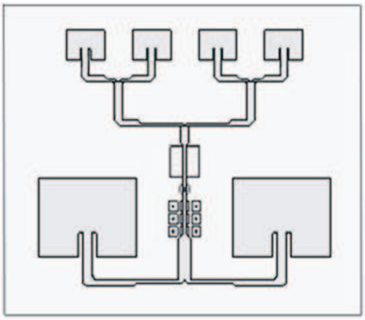

Figure 1. The proposed DbMSAA with mEBG structures located under the feed lines.

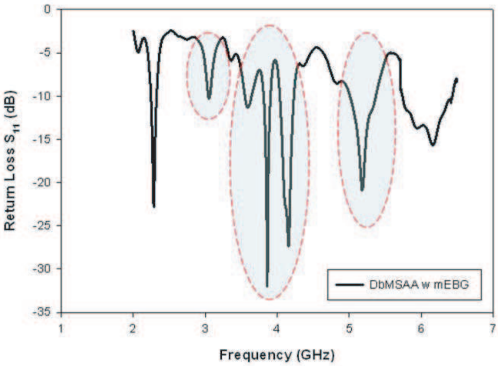

Figure 2. The simulated return loss (dB) for the optimized DbMSAA with mushroom EBG structures, showing a few harmonics in between the resonance frequencies of 2.4 GHz and 5.8 GHz.

incorporating mushroom EBG structures, as shown in Figure 1. On the other hand, there still exist harmonics between the two operating frequencies which radiate and contribute to the losses through the feed networks (Figure 2). Hence, the elimination or reduction of these harmonics using another modified Minkowski EBG structure [2] that exhibits dual band gap characteristic to suppress the unnecessary harmonics, could further improve the radiation characteristics of this antenna.

2. IMPROVED DBMSAA-II DESIGN

The initial configurations of the improved modeled dual band microstrip antenna array are initially designed separately according to their respective frequency of operation at 2.4 GHz and 5.8 GHz, and upon optimization, they were combined to form one array formation. A single sub-miniature version-A (SMA) port is also designed as its main feed connecting the branch of combined non-symmetry corporate inset feed network, as shown in Figure 3. An improvement is done to the first junction of the corporate transmission line feeds where a smooth tapered shaped transmission lines is introduced. Other than that, quarter wave transformers/transmission lines are also introduced connecting the 50 Ohm transmission line feed to the 5.8 GHz patches. These adjustments were introduced to improve and match the impedance thus produce a better return loss at both

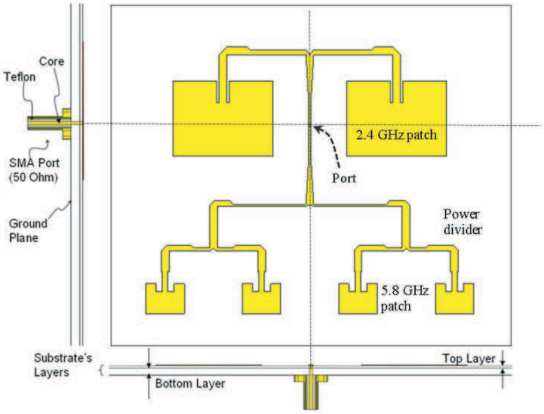

Figure 3. The improved design of the Dual Band Microstrip Antenna Array (DbMSAA-II).

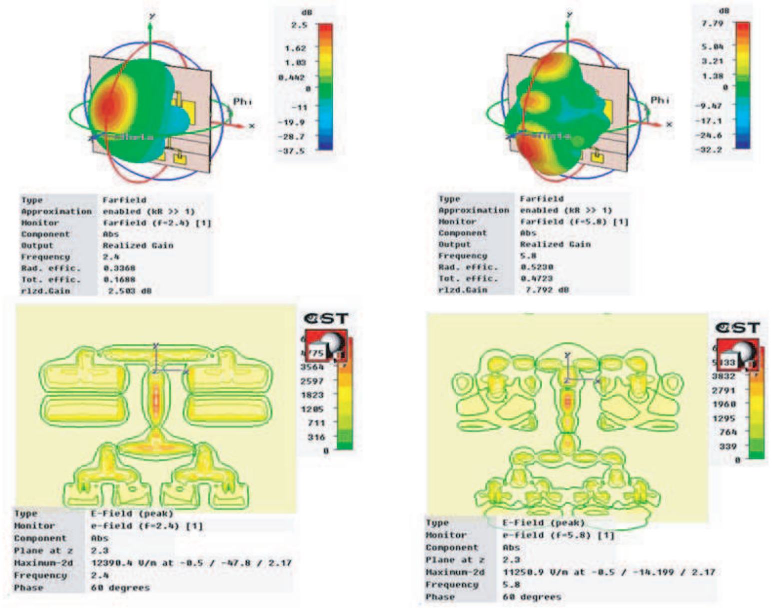

Type	Farfield
Approximation	enabled (kR >> 1)
Monitor	farfield (f=2.4) [1]
Component	Abs
Output	Realized Gain
Frequency	2.4
Rad. effic.	0.3368
Tot. effic.	0.1688
rlzd.Gain	2.503 dB

Type	E-Field (peak)
Monitor	e-field (f=2.4) [1]
Component	Abs
Plane at z	2.3
Maximum-2d	12390.4 V/m at -0.5 / -47.8 / 2.17
Frequency	2.4
Phase	60 degrees

(a)

Type	Farfield
Approximation	enabled (kR >> 1)
Monitor	farfield (f=5.8) [1]
Component	Abs
Output	Realized Gain
Frequency	5.8
Rad. effic.	0.5230
Tot. effic.	0.4723
rlzd.Gain	7.792 dB

Type	E-Field (peak)
Monitor	e-field (f=5.8) [1]
Component	Abs
Plane at z	2.3
Maximum-2d	11250.9 V/m at -0.5 / -14.199 / 2.17
Frequency	5.8
Phase	60 degrees

(b)

Figure 4. The simulated E field and 3D radiation patterns for the improved DbMSAA-II without EBG structures at (a) 2.4 GHz and (b) at 5.8 GHz.

frequencies of operation. The feeding networks and the arrays of radiating patches were printed on the top section of the first single-sided copper clad FR4 board with dielectric constant of 4.6 and a thickness of 1.6 mm. The second/bottom layer, which is also 1.6 mm in thickness and having a full ground plane at the back portion, is needed for incorporation of the EBG structures later on.

For this improved design and without the involvement of the EBG structures, the 5.8 GHz and 2.4 GHz waves and currents were distributed to both the contagious groups of patches through the first junction of the singly fed antenna at the center. On the contrary, these patches were also found to resonate at the contiguous frequencies at different phases. This circumstance degrades the performance especially the radiation patterns of the antenna, at both frequencies. Figure 4 shows the degraded performance of this antenna due to this phenomenon. In the diagram, the E-field distributions of the antenna seems to show that the energy is distributed to both the groups of patches, and all the patch elements are trying to resonate at each other's frequencies. At 5.8 GHz, the developments of the grating lobes are quite severe compared to the lower frequency band of 2.4 GHz as the 2.4 GHz patches have harmonics resonating at 5.8 GHz. Moreover, because the distance between the patches is more than a wavelength vertically, three maximum or grating lobes are generated, as can be seen in Figure 4(b).

3. THE INCORPORATION OF EBG STRUCTURES

Most of the intentions and objectives of the integration of EBG structures with antennas in the literatures [3–12] were either to steer the beam, suppress surface waves or reflect in-phase incident waves in order to improve the performance of the antennas involved. Innovatively, in [1] the mEBG structures that were positioned in between the respective corporate feed lines and ground plane work as Band Rejecter (BR). The EBGs' composition prohibits the propagation of waves of a certain targeted band of frequencies, not including the harmonics in this case, from propagating through them and allows only a certain selected band of frequencies to pass through. In other words, the EBG structures produce a specific 'band gap' characteristics that reject or stop the targeted 'bands' of frequencies of 2.4 GHz or 5.8 GHz and make the respective groups radiate effectively at their own frequencies with full power. In the design, square type of mEBG structures was used. A single $12 \times 12\,\mathrm{mm}^2$ mEBG is used to stop the 2.4 GHz while 3×3 (9 units) of $3\,\mathrm{mm}^2$ mEBG structures, having a gap of 0.5 mm between each other, were used to reject the 5.8 GHz band of frequency. These EBG structures were printed on the second layer (FR4 board) of a thickness of 1.6 mm and were shorted to the ground plane by vertical conducting vias with a radius of 0.4 mm. The vias were positioned at the center of each of the EBG patches, accordingly. The vias plays an important role where without them the EBG structures do not display the band gaps and wave suppression characteristics. The problems faced by the DbMSAA-I were solved through the incorporation of the EBG structures, but further improvements were attempted using another type of EBG structure in this work.

4. DBMSAA INCORPORATED WITH MUSHROOM AND MODIFIED MINKOWSKI EBG STRUCTURES

Referring to Figure 2, the diagram shows the simulated return loss results of the DbMSAA spanning from 1.0 GHz up to 6.5 GHz. It could be observed that in between the two frequencies of operation of 2.40 GHz and 5.80 GHz, there still exist a few harmonics which, if suppressed, might improve the performance of the antenna further. From the simulations carried out, it was found that the junction leading to the 5.8 GHz elements produced these harmonics. Thus, the modified Minkowski EBG structures as designed in [2] are proposed and incorporated, replacing the single square $12 \times 12\,\text{mm}^2$ mushroom EBG at the junction, to perform the harmonics reduction as intended. The 9 units of $3 \times 3\,\text{mm}^2$ at the other junction leading to the 2.4 GHz

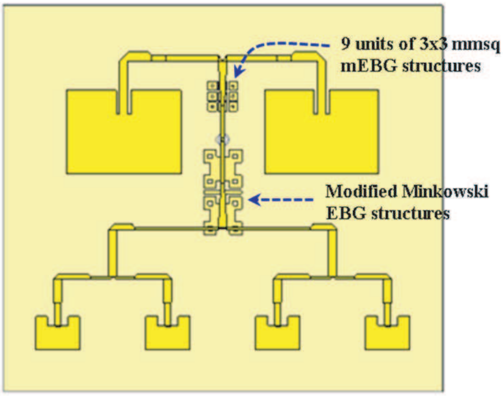

Figure 5. The DbMSAA-II incorporated with the combination of 9 units of $3 \times 3\,\text{mm}^2$ mEBG structures and modified Minkowski EBG structures.

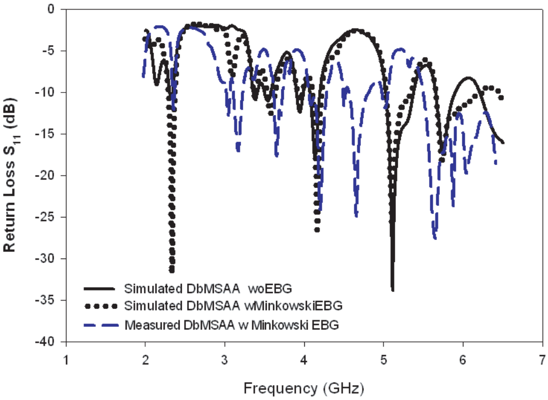

Figure 6. Return Loss (S_{11}) results comparison between the simulated and measured DbMSAA-II, without and with mEBG and Minkowski EBG structures.

elements are maintained. Figure 5 shows the DbMSAA-II with the combination of the mEBG and modified Minkowski structures, and Figure 6 depicts the simulated return loss results.

5. RESULTS AND DISCUSSIONS

The possibilities of having a uniform and controlled radiation patterns and improved antenna's performance are achieved and realized through the incorporation of the EBG structures. The antenna's performance is improved where the radiation patterns become more symmetrical, especially at 5.8 GHz as shown in the simulated results in Figures 7(a) and (b).

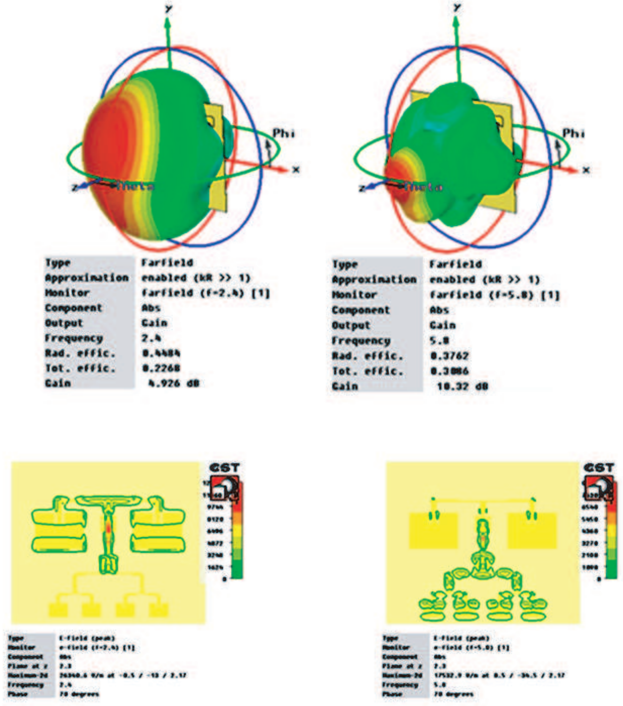

Type	Farfield
Approximation	enabled (kR >> 1)
Monitor	farfield (f=2.4) [1]
Component	Abs
Output	Gain
Frequency	2.4
Rad. effic.	0.4484
Tot. effic.	0.2268
Gain	4.926 dB

Type	Farfield
Approximation	enabled (kR >> 1)
Monitor	farfield (f=5.8) [1]
Component	Abs
Output	Gain
Frequency	5.8
Rad. effic.	0.3762
Tot. effic.	0.3086
Gain	10.32 dB

Type	E-field (peak)
Monitor	e-field (f=2.4) [1]
Component	Abs
Plane at z	2.3
Maximum-2d	26340.6 V/m at -0.5 / -13 / 2.17
Frequency	2.4
Phase	70 degrees

Type	E-field (peak)
Monitor	e-field (f=5.8) [1]
Component	Abs
Plane at z	2.3
Maximum-2d	17532.9 V/m at 0.5 / -34.5 / 2.17
Frequency	5.8
Phase	70 degrees

(a) (b)

Figure 7. The *E* fields were distributed appropriately to the respective elements after the incorporation of mEBG and the modified Minkowski EBG structures at the strategic positions. (a) At 2.40 GHz and (b), at 5.80 GHz.

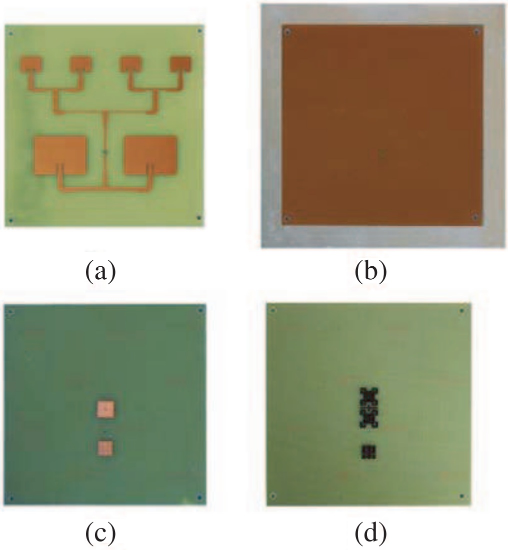
(a) (b)

(c) (d)

Figure 8. The fabricated DbMSAA-II with the EBG structures' designs. (a) The top layer that consists of the DbMSAA's feed networks and respective radiating elements; (b) A plain FR4 dielectric substrate without EBG structures. (c) mEBG structures (d) Minkowski and mEBG structures.

The respective groups of elements resonate efficiently at their own respective frequencies, simultaneously. This also resulted in the elimination of the grating lobes at 5.8 GHz. The powers were also effectively distributed to the respective junctions thus increased the gain of the antennas involved. Without EBG structures, the simulated realized gain at 2.4 GHz is about 2.5 dB and at 5.8 GHz is 7.80 dB. With the incorporation of the EBG structures, the gain increases to 4.93 dB and 10.32 dB for the 2.4 GHz and 5.8 GHz antennas, respectively. The side lobes remaine even after the incorporation of the EBG structures, and it is due to the spurious radiation from the feed networks. This problem is not as serious as it seems when the performance of the antenna has been improved. Different feed networks and techniques could eliminate this problem and does not necessarily involve the integration of EBG structures, but the design is more complex.

The diagrams in Figure 8 show the fabricated antennas' main components where (a)is the top layer that consists of the DbMSAA-II's feed networks and respective radiating elements, (b) the plain FR4 dielectric substrate (without EBG structures for comparison purposes) over the aluminum ground plane, (c) the mushroom EBG structures, (d) the combination of mushroom and modified Minkowski EBG structures. All of the antennas were attached to the aluminum ground plane as their base. Figure 9 and Figure 10 show the measured *E* and *H* plane cuts of the fabricated DbMSAA-I and DbMSAA-II without and with the respective EBG structures.

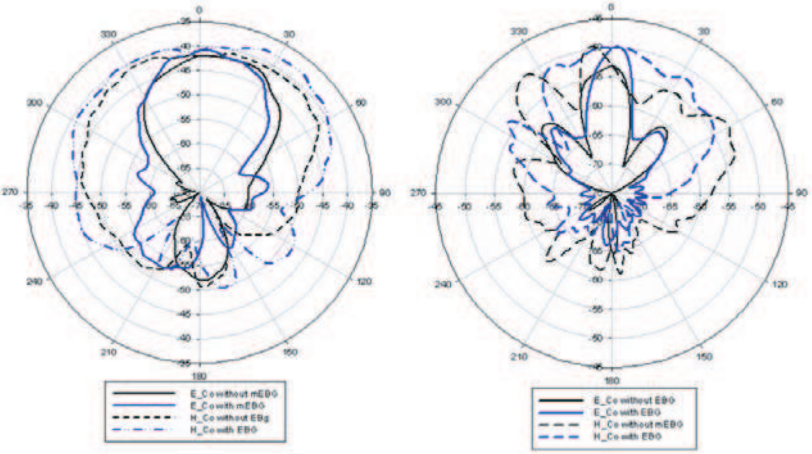

(a) (b)

Figure 9. Measured *E* & *H* plane cuts for the DbMSAA-I with and without Mushroom EBG structures (a) at 2.4 GHz and (b) at 5.8 GHz.

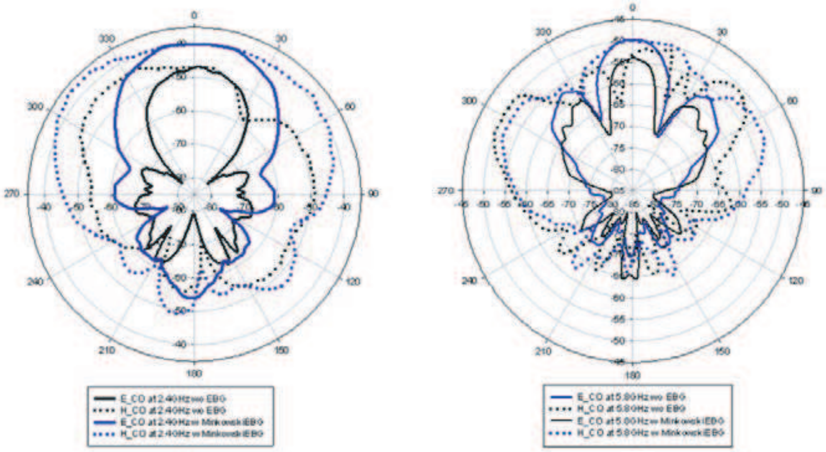

(a) (b)

Figure 10. Measured *E* & *H* plane cuts for the DbMSAA-II with and without the combination of mushroom and the modified Minkowski EBG structures (a) at 2.4 GHz and (b) at 5.8 GHz.

Table 1 presents the summarized details of the antennas' performance. From this table, it is observed that the DbMSAAs' performances have been improved spectacularly when integrated with the EBG structures. The DbMSAA-I, incorporated with Mushroom EBG structures, shows a smaller E and H planes' HPBW at 2.4 GHz. At 5.8 GHz, its E plane's HPBW also shows a little decrement, but this results in the wider H plane's beamwidth at this frequency. The DbMSAA-II, incorporated with the modified Minkowski EBGs and combined with the 3×3 units of $3.0\,\mathrm{mm}^2$ mEBG structures, shows an increment of their E and H planes' HPBW for both frequencies.

Table 1. A comparison of the E and H planes' Half Power Beam Width (HPBW) for DbMSAA-I and DbMSAA-II.

Type of Antenna & EBG	**Antenna (f_r)**	***E* Plane (HPBW)**	***H* Plane (HPBW)**
DbMSAA-I Mushroom & Mushroom	without EBG (2.40 GHz)	60.0°	125.0°
	with EBG (2.40 GHz)	50.0°	117.0°
	without EBG (5.80 GHz)	19.0°	Gl ∼ 18.0°
	with EBG (5.80 GHz)	9.5°	72.0°
DbMSAA-II Mushroom & Minkowski	without EBG (2.40 GHz)	40°	60°
	with EBG (2.40 GHz)	84°	113°
	without EBG (5.80 GHz)	13°	Gl ∼ 25°
	with EBG (5.80 GHz)	26°	40°

Note: Gl = Grating lobe (max)

6. CONCLUSION

New Dual band Microstrip Antenna Arrays (DbMSAA), consisting of two different groups of radiating elements working at two different frequencies of operation at 2.4 GHz & 5.8 GHz and incorporated with different types of EBG structures, have been designed and analyzed. Their performance has been improved with the incorporation of the EBG structures that act as band rejecters at the specific junctions. The grating lobes at 5.8 GHz diminish, and the radiation patterns of the dual band antenna at both frequencies become more symmetrical with increased gain. This antenna is suitable for point-to-point and point to multi-point Dual-Band Wireless LAN/next generation IEEE 802.11n wireless communication systems' applications, which works at both the U-NII/ISM band of frequencies, simultaneously.

ACKNOWLEDGMENT

The authors thank the Ministry of Science, Technology and Innovation (MOSTI) of Malaysia, Research Management Center (RMC), UTM and the Faculty of Electrical Engineering for supporting this research.

REFERENCES

1. Masri, T., M. K. A. Rahim, and O. Ayop, "Dual band microstrip array antenna radiation characteristics enhancement via novel band rejection technique using EBG structures," *2008 Asia Pacific Microwave Conference, (APMC 2009)*, December 2008.
2. Masri, T., M. K. A. Rahim, and M. N. A. Karim, "A novel 2D Minkowski gasket EBG structure for multiband microstrip antenna," *European Conference on Antenna and Propagation (EuCAP 2007)*, Edinburgh, U.K., November 11–16, 2007.
3. Yang, F. and Y. Rahmat-Samii, *Electromagnetic Band Gap Structures in Antenna Engineering*, Cambridge University Press, 2009.
4. Yang, L., M. Fan, F. Chen, J. She, and Z. Feng, "A novel compact electromagnetic-bandgap (EBG) structure and its application for microwave circuits," *IEEE Transaction on Microwave Theory and Techniques*, Vol. 53, No. 1, January 2005.
5. Yang, F. and Y. Rahmat-samii, "Microstrip antennas integrated with electromagnetic band-gap (EBG) structures: A low mutual coupling design for array applications," *IEEE Transaction on Antennas and Propagation*, Vol. 51, No. 10, 2936–2946, 2003.
6. Diaz, R., V. Sanchez, E. Caswell, and A. Miller, "Magnetic loading of artificial magnetic conductors for bandwidth enhancement," *IEEE Antennas and Propagation Society International Symposium*, Vol. 2, 431–434, 2003.
7. Du, Z. W., K. Gong, J. S. Fu, B. X. Gao, and Z. H. Feng, "A compact planar inverted-F antenna with a PBG-type ground plane for mobile communication," *IEEE Transaction on Vehicular Technology*, Vol. 52, No. 3, 483–489, 2003.
8. Sievenpiper, D. and J. H. Schauffner, "Textured surface having high electromagnetic impedance in multiple frequency bands," U.S. Patent 6,483,481, November 19, 2002.
9. Broas, R. F. J., D. F. Sievenpiper, and E. Yablonovitch, "A high-impedance ground plane applied to a cellphone handset geometry," *IEEE Transaction on Microwave Theory and Techniques*, Vol. 49, No. 7, 1262–1265, 2001.

10. Pirhadi, A., M. Hakak, and F. Keshmiri, "Using electromagnetic band gap superstrate to enhance the bandwidth of probe-fed microstrip antenna," *Progress In Electromagnetic Research*, PIER 61, 215–230, 2006.
11. Shaban, H. F., H. A. Elmikatay, A. A. Shaalan, "Study the effects of electromagnetic band-gap (EBG) substrate on two patches microstrip antenna," *Progress In Electromagnetic Research B*, Vol. 10, 55–74, 2008.
12. Zhang, L.-J., C.-H. Liang, L. Liang, and L. Chen, "A novel design approach for dual band electromagnetic band gap structure," *Progress In Electromagnetic Research M*, Vol. 4, 81–91, 2008.